ECCM

20

26-30 JUNE

2022

LAUSANNE

SWITZERLAND

Proceedings of the 20th European Conference on Composite Materials

COMPOSITES MEET SUSTAINABILITY

Vol 2 – Manufacturing

Editors : Anastasios P. Vassilopoulos, Véronique Michaud

Organized by :

EPFL

Under the patronage of :

CCLAB Composite Construction Laboratory

LPAC Laboratory for Processing of Advanced Composites

ESCM EUROPEAN SOCIETY FOR COMPOSITE MATERIALS

ECCM 20
26-30 JUNE 2022
LAUSANNE SWITZERLAND

EPFL CCLAB Composite Construction Laboratory LPAC Laboratory for Processing of Advanced Composites

Proceedings of the 20th European Conference on Composite Materials ECCM20 26-30 June 2022, EPFL Lausanne Switzerland

Edited By :

Prof. Anastasios P. Vassilopoulos, CCLab/EPFL
Prof. Véronique Michaud, LPAC/EPFL

Oragnized by:

Composite Construction Laboratory (CCLab)
Laboratory for Processing of Advanced Composites (LPAC)
Ecole Polytechnique Fédérale de Lausanne (EPFL)

ISBN: 978-2-9701614-0-0
DOI: http://dx.doi.org/10.5075/epfl-298799_978-2-9701614-0-0

Published by :

Composite Construction Laboratory (CCLab)
Ecole Polytechnique Fédérale de Lausanne (EPFL)
BP 2225 (Bâtiment BP), Station 16
1015, Lausanne, Switzerland

https://cclab.epfl.ch

Laboratory for Processing of Advanced Composites (LPAC)
Ecole Polytechnique Fédérale de Lausanne (EPFL)
MXG 139 (Bâtiment MXG), Station 12
1015, Lausanne, Switzerland

https://lpac.epfl.ch

Cover:

Swiss Tech Convention Center
© Edouard Venceslau - CompuWeb SA

Cover Design:

Composite Construction Laboratory (CCLab)
Ecole Polytechnique Fédérale de Lausanne (EPFL)
Lausanne, Switzerland

©2022 ECCM20/The publishers

Disclaimer:

The ECCM20 organizing committee and the Editors of these proceedings assume no responsibility or liability for the content, statements and opinions expressed by the authors in their corresponding publication.

Editorial

This collection gathers all the articles that were submitted and presented at the 20th European Conference on Composite Materials (ECCM20) which took place in Lausanne, Switzerland, June 26-30, 2022.

ECCM20 is the 20th edition of a conference series having its roots back in time, organized each two years by members of the European Society of Composite Materials (ESCM).

The ECCM20 event was organized by the Composite Construction laboratory (CCLab) and the Laboratory for Processing of Advanced Composites (LPAC) of the Ecole Polytechnique Fédérale de Lausanne (EPFL).

The Conference Theme this year was “Composites meet Sustainability”. As a result, even if all topics related to composite processing, properties and applications have been covered, sustainability aspects were highlighted with specific lectures, roundtables and sessions on a range of topics, from bio-based composites to energy efficiency in materials production and use phases, as well as end-of-life scenarios and recycling.

More than 1000 participants shared their recent research results and participated to fruitful discussions during the five conference days, while they contributed more than 850 papers which form the six volumes of the conference proceedings. Each volume gathers contributions on specific topics:

Vol 1 – Materials

Vol 2 – Manufacturing

Vol 3 – Characterization

Vol 4 – Modeling and Prediction

Vol 5 – Applications and Structures

Vol 6 – Life Cycle Assessment

We enjoyed the event; we had the chance to meet each other in person again, shake hands, hold friendly talks and maintain our long-lasting collaborations. We appreciated the high level of the research presented at the conference and the quality of the submissions that are now collected in these six volumes. We hope that everyone interested in the status of the European Composites’ research in 2022 will be fascinated by this publication.

The Conference Chairs

Anastasios P. Vassilopoulos, Véronique Michaud

FRACTURE TOUGHNESS AND PERFORMANCE OF RESISTANCE-WELDED AND CO-BONDED THERMOSET/THERMOPLASTIC POLYMER COMPOSITE HYBRID JOINTS

Thomas, Maierhofer[*,a]*, Evripides G., Loukaides*[a]*, Thibault, Hernandez*[b]*, Craig, Carr*[c]*,*
Chiara, Bisagni[d]*, and Richard, Butler*[a]

a: Materials and Structures Centre, Dept. of Mechanical Engineering, University of Bath, UK
b: The ThermoPlastic Composites Research Centre, Netherlands
c: GKN Aerospace, Global Technology Centre, UK
d: Delft University of Technology, Faculty of Aerospace Engineering, Netherlands
*Corresponding author's e-mail: tam48@bath.ac.uk

Abstract: *Modern aerospace structures see increasing use of combinations of thermoplastic and thermoset composite components, requiring the development of efficient joining methods for dissimilar matrix materials. This study aimed to investigate the Mode I fracture toughness and performance of resistance-welded and co-bonded thermoset-thermoplastic composite joints for primary aerospace structural applications. Double cantilever beam and single lap shear trials were performed. It was found that using resistance welding, a significant improvement in the Mode I fracture toughness of approximately 360 % - 520 % over co-bonding can be achieved. Single lap shear tests did not allow any conclusion about the bond strengths due to thermoset laminate failure. Although, combined with optical microscopy of the fracture surfaces, it was possible to show that significant thermal degradation of the thermoset matrix can be avoided.*

Keywords: Hybrid joints; resistance welding; co-bonding; fracture toughness; thermoset-thermoplastic

1. Introduction

For improved design flexibility and structural efficiency, there is a growing interest in using a combination of thermoset composite (TSC) and thermoplastic composite (TPC) components for aerospace structures. Taking advantage of their different properties allows for increased design flexibility and further structural optimisation [1]. One of the main challenges is the efficient joining of composite components. Amongst other factors, structural efficiency, ease and cost of assembly, repairability and stringent certification regulations drive the selection of joining processes for aerospace applications [2].

Mechanical fastening and adhesive bonding are most commonly used for the assembly of TSC and TPC components. Mechanical fastening however is suboptimal for joining CFRP parts as fastener holes create stress concentrations or need complex fibre steering, add a significant amount of weight and require additional sealing [3]. The structural efficiency of thermoset adhesive joints is inherently better and they are much lighter than mechanically fastened joints. Though, thermoset adhesives often require long curing cycles, are permanent, cannot easily be repaired in field operations and require extensive surface preparation [4]. The performance of a bond is highly dependent on proper surface preparation. Current nondestructive inspection methods can detect voids and debonds. However, they cannot detect weak bonds (zero-volume debonds), thus making it difficult to predict the bond performance [5]. An alternative joining

  doi:10.5075/epfl-298799_978-2-9701614-0-0

method that can be readily applied to TPC is fusion bonding (welding). It offers significantly reduced cycle times and eliminates complex surface preparation whilst offering similar joint strength to traditional joining methods [6]. To make a TSC weldable, an established concept is to co-bond a thermoplastic film with an uncured TSC. Previous studies performed by Villegas et al. [7] have demonstrated that if the thermoset resin and thermoplastic coupling layer (CL) are chemically compatible and initially miscible, a reaction induced gradient diffused interface (interphase) forms. This interphase results in a strong bond between the thermoset resin and the CL via molecular entanglements [4]. Polyetherimide (PEI) is a strong candidate for the CL material for primary structural applications due to its compatibility with polyaryletherketones (PAEKs) and commonly used epoxy resins [7]. One of the most promising fusion bonding methods for joining TSC-TPC components is resistance welding. Ageorges et al. [8] and Zweifel et al. [9] have previously studied the applicability of resistance welding for creating TSC-TPC hybrid joints using single lap shear (SLS) tests. However, very limited research exists on the fracture toughness and performance of bonded TSC-TPC joints for aerospace applications.

This study focused on the evaluation and comparison of the Mode I fracture toughness of resistance-welded (RW) and co-bonded (CB) TSC-TPC hybrid joints, by conducting double cantilever beam (DCB) tests. Furthermore, SLS samples were tested to assess joint performance.

2. Experimental procedure

2.1 Manufacturing of adherends and heating elements

In this study, two different types of aerospace-grade carbon fibre reinforced TPC and one carbon fibre reinforced TSC were used. Both thermoplastic laminates consisted of 16-plies with a stacking sequence of $[0/90/0/90/0_3/90]_s$. A Cetex® TC1225/T700 laminate, with a low-melt PAEK matrix, was supplied by Toray Advanced Composites. The laminate was manufactured using a hot platen press, with a consolidated mean laminate thickness of 2.2 mm. APC® PEKK-FC/AS4D, with a polyetherketoneketone matrix, prepreg was supplied by Solvay and consolidated using the manufacturer's recommended autoclave cycle, by maintaining the maximum temperature of 377 °C at a pressure of 0.7 MPa for 20 min, resulting in a consolidated mean laminate thickness of 2.3 mm.

Thermoset laminates were made of 11-plies HexPly® AS4/8552 (CF/epoxy) with a stacking sequence of $[0/90/0/90/0/\underline{0}]_s$, tailored to match the bending stiffness of thermoplastic laminates. CF/epoxy laminates were autoclave cured using the manufacturer's recommended cycle by maintaining a maximum temperature of 180 °C under 0.7 MPa pressure for 120 min, with a cured laminate thickness of 2.2 mm. For thermoset laminates used for resistance welding, a 250 µm-thick PEI film (grade ULTEM 1000) was co-bonded on one surface with the uncured CF/epoxy. This created a thermoplastic rich, weldable surface. A strong bond between the epoxy matrix and the PEI film was formed via molecular entanglements resulting in a gradient thermoset-thermoplastic polymer interphase with a thickness of approximately 30 µm. The interphase thickness was measured on cross-section samples of co-bonded CF/epoxy-PEI laminates using optical microscopy (OM), as shown in figure 2.a.

For resistance welding, two different heating elements (HEs) were investigated. The primary HE used consists of a woven stainless steel (SS) mesh, with a wire thickness of 40 µm and an open gaps size of 87 µm, sandwiched between two plies of 8-harness satin weave glass fibre (GF) TC1225/EC6 (GF/PAEK), from Toray Advanced Composites. The second HE (uninsulated HE)

investigated consists of the same woven SS mesh sandwiched between two 50 µm thick PEI films (ULTEM 1000). This was only used to establish the feasibility of using an uninsulated HE. Both HEs were consolidated in a hot platen press at 350 °C under a pressure of 1.0 MPa for 20 min.

2.2 Adhesive co-bonding

Thermoset and thermoplastic laminates were cut into 200 mm x 155 mm panels for DCB samples and 300 mm x 101.6 mm panels for SLS samples. Thermoplastic laminates were mechanically abraded and surface wet wiped using Isopropyl alcohol, followed by Argon plasma treatment, using an atmospheric plasma torch. A 3M™ Scotch-Weld™ AF 555M epoxy film, with a thickness of 200 µm was used for co-bonding the uncured CF/epoxy laminate and the plasma-treated thermoplastic laminates. To minimise exposure of the surface-treated laminates, adhesive bonding was performed immediately after plasma treatment. Co-bonded hybrid joints were then cured in an autoclave, maintaining a maximum temperature of 180 °C and 0.2 MPa pressure for 120 min. As a pre-crack initiator for DCB samples, a 13 µm thick PTFE film was inserted at the joint interface between the epoxy film and the thermoset adherend. Figures 1.a and 1.b show an illustration and an OM image of the joint cross-section of co-bonded samples.

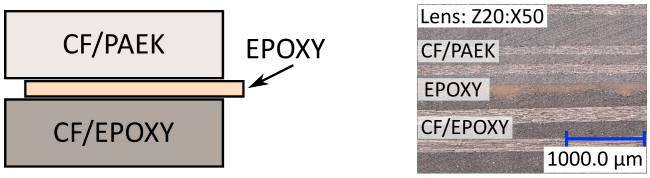

Figure 1. Co-bonded samples: (a) illustration of joint, (b) OM cross-section of joint.

2.3 Resistance welding

Resistance welding was performed at the ThermoPlastic composites Research Center (TPRC), NL, using an in-house developed welding rig. The power was supplied via a computer-controlled 6 kW power supply unit with a maximum DC voltage output of 45 V and a maximum current output of 140 A. The welding and clamping pressure to hold the specimen and connect the power source to the HE were provided via pneumatic actuators. The pressure was uniformly distributed across the specimens' surfaces via active air-cooled aluminium blocks. For DCB specimens, laminates were cut into 250 mm x 50 mm strips, with a heating element width of 25 mm and for SLS specimens laminates were cut into 250 mm x 101.6 mm adherends with a welded overlap of 25.4 mm. To introduce a pre-crack in DCB coupons, a 13 µm thick polyimide film was placed at the interface between the CF/epoxy adherend and the HE, as the crack propagation between the CF/epoxy and the PAEK matrix of the HE was investigated. In figure 2.a an illustration and in figure 2.b an OM image of the cross-section of welded samples is shown.

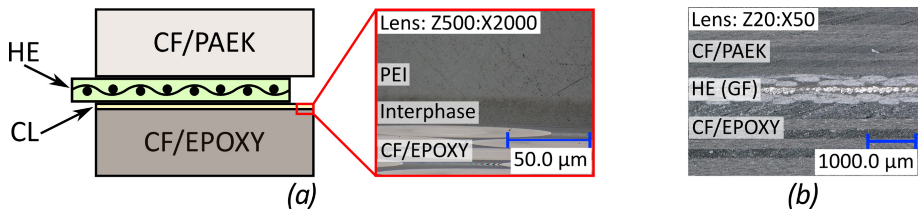

Figure 2. RW samples: (a) joint illustration and OM of interphase, (b) OM cross-section of joint.

To monitor the welding process and ensure fully welded joints, for every performed weld a K-type thermocouple was placed at the HE/CL interface, outside the specimen test region.

Additional welds were performed to determine the optimum welding parameters for the GF insulated HE. These welds had six K-type thermocouples bonded between the PEI CL and the thermoset laminate and two further K-type thermocouples placed between the HE and the PEI CL. To evaluate the applicability of an uninsulated HE, additional layers of 50 µm PEI film were added up to a total thickness of 350 µm on either side of the HE, aiming to prevent current leakage to the laminate. However, this was unsuccessful and current leaking to the fibres of the adherent could not be prevented. Therefore, achieving a uniform weld was impossible. Hence, only the primary GF insulated heating elements were used for producing the specimens. For the manufacturing of DCB and SLS specimens process parameters were chosen to achieve rapid heating of the interface to 350 °C and to maintain it for 30 s, ensuring a fully welded joint. This was achieved via a high initial current of 45 A which was reduced to approximately 30 A once the interface temperature reached 350 °C. The welding cycle is illustrated in figures 3.a and 3.b.

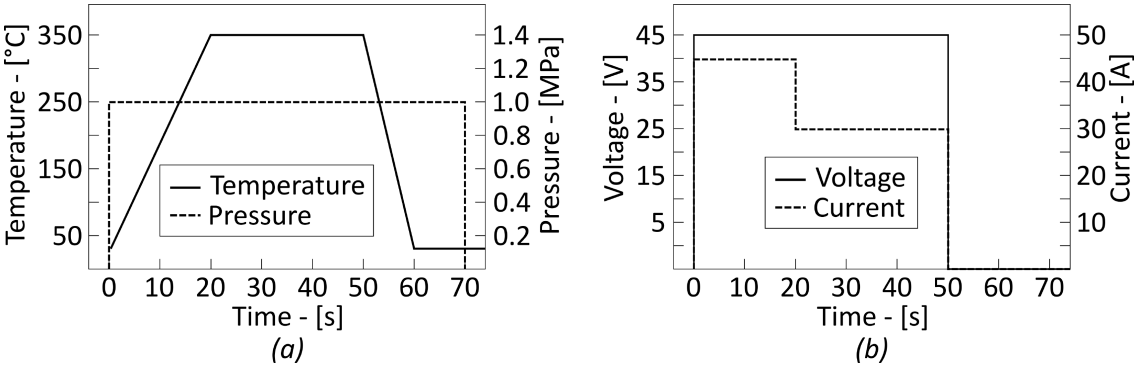

Figure 3. Resistance welding target cycle parameters: (a) interface temperature and welding pressure, (b) power supply: voltage and current.

2.4 Testing and performance analysis

SLS and DCB experiments were based on ASTM D5868 and ASTM D5528 standards respectively. SLS samples were cut into 25.4 mm wide specimens. DCB samples were cut into 160 mm x 21 mm specimens with a crack insert length of 52.5 mm. Tests were performed using an Instron 50 kN universal testing machine. For SLS and DCB specimens, load rates of 13 mm/min and 1 mm/min respectively were chosen, with all tests performed in standard laboratory conditions (23 °C and 50 % relative humidity). For all samples, the force and crosshead displacement of the testing machine were recorded. The side faces of DCB specimens were spray-painted with a thin layer of white acrylic paint. Crack front propagation on DCB specimens was recorded by bonding crack length gauges, with an accuracy of ±0.5 mm to both specimen side faces and recording crack growth using a 4K camera. For SLS samples, seven welded and five co-bonded specimens were tested per material combination. Six DCB tests were performed for each coupon configuration.

Lap shear strengths (LSS) were calculated by dividing the failure load by the bonded joint area of SLS experiments. The Mode I fracture toughness (G_{IC}) was calculated using the modified beam theory method, as it was observed to yield the most conservative fracture toughnesses for the majority of tested samples [10]. The Mode I fracture toughness was therefore calculated using:

$$G_{IC} = \frac{3P\delta}{2b(a+|\Delta|)} \quad (1)$$

The modified beam theory method accounts for the rotation at the crack front by increasing the crack length (a) to $a + |\Delta|$. Δ was determined for each specimen by creating a least-squares fit of the cube root of the compliance ($C^{1/3}$) against crack length, where C is the ratio of load point displacement vs. applied load.

3. Results and discussion

3.1 Lap shear strength

Lap shear strength values showed similar performance values for both hybrid co-bonded and hybrid resistance-welded samples, as outlined in table 1 and shown in figure 4.

Table 1: LSS, standard deviation (SD) and coefficient of variation (CV) of each sample type.

Sample type	LSS – [MPa]	SD – [MPa]	CV – [%]
CB-LMP	7.7	0.6	8.3
CB-PEKK	9.6	1.6	16.3
RW-LMP	11.7	0.9	8.1
RW-PEKK	10.2	1.5	15.1

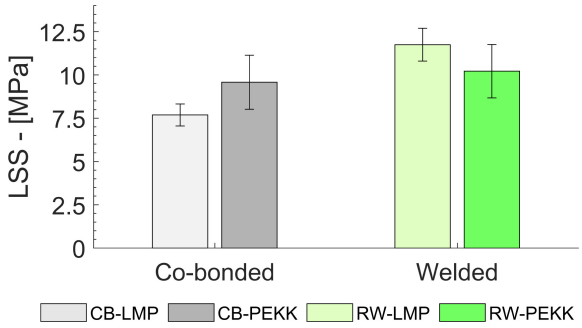

Figure 4. LSS comparison between co-bonded and resistance-welded hybrid joints.

The observed failure mode for all specimens, independent of coupon configuration was laminate failure between the first and second ply (0/90) interface of the thermoset adherend. As a result, the performed SLS tests do not allow any conclusion about the actual bond strength, apart from the joint being stronger than the thermoset laminate's interfacial strength. However, given that the heat-affected zone is focused around the joint interface, CF/epoxy plies closest to the joint interface are subject to the greatest risk of thermal degradation. Hence, as the observed LSS for CB and RW samples are comparable and failure occurred between the 1st and 2nd ply, it is concluded that thermal degradation of the thermoset matrix was successfully prevented.

3.2 Mode I fracture toughness

The main focus of this study was to investigate and compare the Mode I fracture toughness of resistance-welded vs. co-bonded TSC-TPC hybrid joints. Post bonding optical microscopic analysis showed that, due to resin flow during the bonding process, insert folds at the crack tip formed in most specimens. Therefore, specimens were loaded to an initial increment of crack growth, unloaded, and then reloaded to induce crack growth from a natural Mode I pre-crack.

For fracture toughness analysis, only G_{IC} values obtained from reloading cycles were evaluated. Table 2 and figure 5.a show the obtained mean initiation ($G_{IC,INIT.}$) and propagation ($G_{IC,PROP.}$) toughnesses, SDs and CVs for each sample type respectively. Example R-curves for a CB-LMP specimen and a RW-LMP specimen are shown in figure 5.b.

Table 2: Mean G_{IC} initiation and propagation toughnesses with respective SDs and CVs.

Sample type	$G_{IC,INIT.}$ – [J/m²]	SD– [J/m²]	CV – [%]	$G_{IC,PROP.}$ – [J/m²]	SD – [J/m²]	CV – [%]
CB-LMP	267	14.0	5.2	301	15.7	5.2
CB-PEKK	399	74.0	18.5	450	73.8	16.4
RW-LMP	1650	241.0	14.6	2097	242.7	11.6
RW-PEKK	1847	177.9	9.6	2246	129.9	5.8

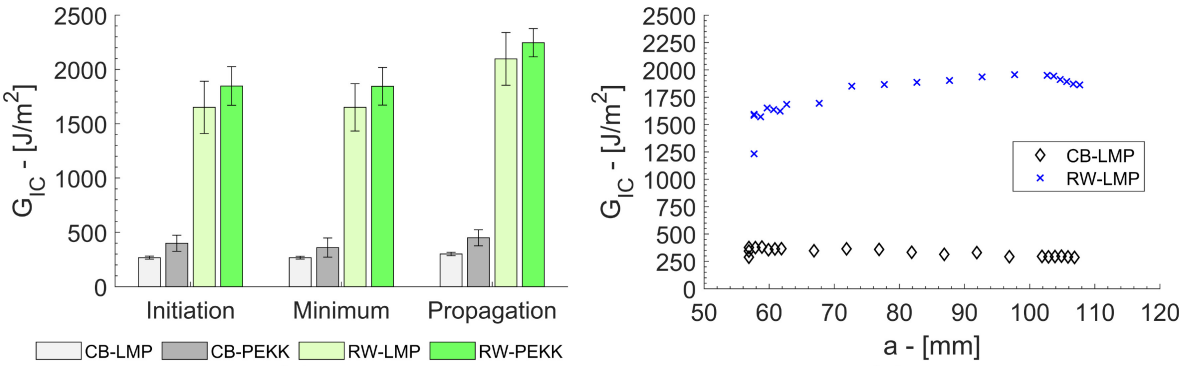

Figure 5. (a) Initiation, minimum and propagation G_{IC} values with respective SDs for all samples, (b) example R-curves for co-bonded and resistance-welded specimens.

In comparison to co-bonded joints, the resistance-welded joint interface is much more complex, as it consists of multiple different material systems. Thus, it is much more challenging to evaluate the fracture toughness for a specific joint configuration. However, resistance-welded samples show a Mode I fracture toughness increase of approximately 360 % - 520 % vs. co-bonded samples. This suggests that resistance welding may offer a significant performance improvement in addition to a much shorter manufacturing cycle time when compared to adhesive bonding.

The main failure mode of co-bonded samples was adhesive failure between the epoxy film adhesive and the thermoplastic adherend with partial thin layer cohesive failure being observed along the fracture surface. For most CB samples, a run-arrest crack extension was observed.

For welded samples, as the pre-crack insert was placed at the HE/CL interface, it was expected that the crack would propagate at that interface, with a risk of it extending into the thermoset laminate. Though in general, crack extension tended towards the midplane of the joint, which resulted in significant fibre bridging between the HE's GF insulation and the CL over a distinct length of crack extension. Fibre bridging significantly increased the local fracture toughnesses at a given crack length, as the load was partially transferred to the bridged GFs. This phenomenon is reflected in the R-curve shown in figure 6.a, with figure 6.b showing an example of fibre

  doi:10.5075/epfl-298799_978-2-9701614-0-0

bridging occurring shortly after crack initiation. The resulting toughness extrema were excluded from the data used to evaluate mean toughness values. Even though most specimens showed fibre bridging to some degree, due to the phenomenon being limited to a distinct crack extension, it is believed that the "true" Mode I fracture toughness can be extracted where no fibre bridging was visually observed. The primary failure modes observed were the cohesive failure of the CL and fibre-tear failure of the HE. Although initial results are promising further tests are recommended to determine whether an offset of the pre-crack insert from the joint mid-plane resulted in structural coupling hence resulting in mixed mode failure.

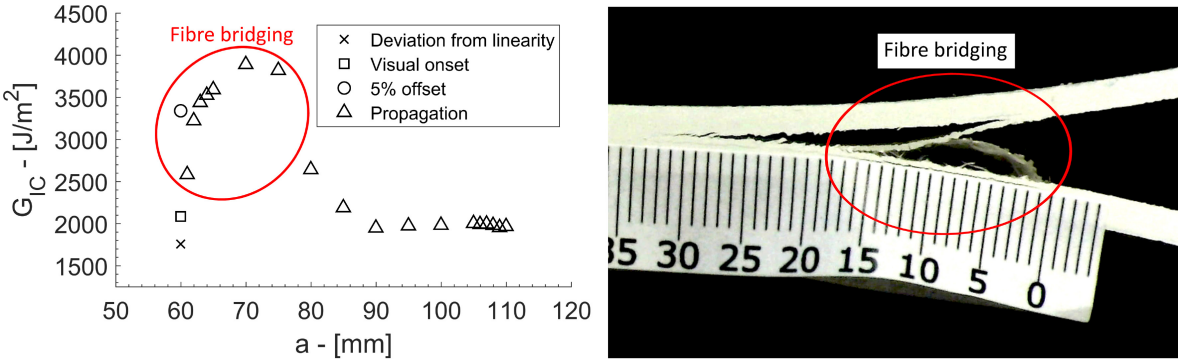

(a) *(b)*

Figure 6. (a) R-curve showing the effect of fibre bridging on G_{IC}, (b) fibre bridging between GF insulation of the HE and thermoplastic CL.

Two RW-PEKK specimens were exposed to prolonged high power heating, resulting in exceeding the required processing temperature and reaching interface temperatures above 500 °C. As a result, the epoxy matrix was expected to show signs of thermal degradation. Optical microscopy of the fracture surface allowed the identification of discoloured resin and a significant amount of epoxy sublimation-induced porosity trapped in the consolidated thermoplastic resin pool. Figures 7.a and 7.b show an extract of the fracture surface of both an overheated specimen and another produced following the target welding cycle shown in figure 3 respectively. Overheating resulted in a significant fracture toughness reduction of approximately 80 % (≈450 J/m^2).

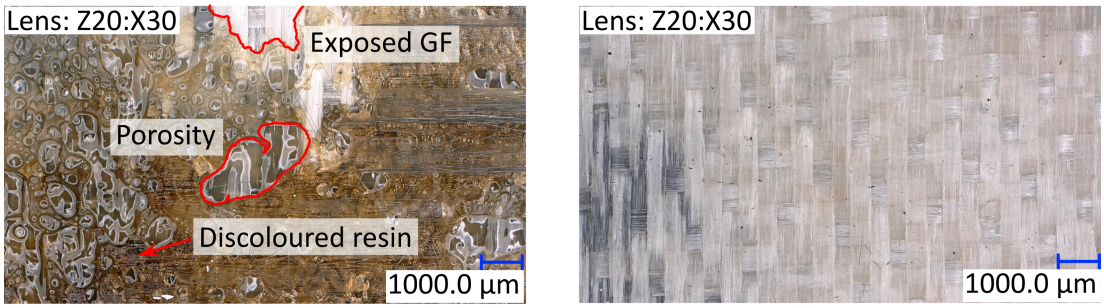

(a) *(b)*

Figure 7. RW DCB fracture surface: (a) overheated specimen, (b) target cycle specimen.

Conclusion

An experimental study on the Mode I fracture toughness and joint performance of co-bonded and resistance-welded thermoset-thermoplastic composite hybrid joints was performed. Four different sample configurations were investigated: two co-bonded (CB-LMP and CB-PEKK) and two resistance-welded (RW-LMP and RW-PEKK). Single lap shear tests were performed for which laminate failure was observed for all tested specimens. However, because the laminate failure

occurred between the first and second ply and comparable lap shear strengths were obtained for both joining methods, it is concluded that thermal degradation of the thermoset adherend can be avoided. When comparing resistance-welded with co-bonded samples, the obtained Mode I fracture toughness for resistance-welded samples were evaluated to be approximately 360 % - 520 % higher. However, failure of resistance-welded joints is much more complex, potentially making it difficult to achieve pure Mode I fracture.

Acknowledgements

The authors gratefully acknowledge GKN Aerospace UK for their continuous support and industrial guidance. Technical advice and manufacturing assistance provided by the ThermoPlastic composites Research Center (TPRC), NL, the Advanced Manufacturing Research Centre (AMRC), UK, and the National Composites Centre (NCC), UK, are greatly appreciated. The authors want to thank Toray Advanced Composites and Solvay for supplying the thermoplastic laminates and prepreg. Richard Butler holds the Royal Academy of Engineering - GKN Aerospace Research Chair. The research was gratefully supported by the EPSRC, UK, Programme Grant: "Certification for Design: Reshaping the Testing Pyramid" (CerTest, EP/S017038/1).

4. References

1. Quan D, Alderliesten R, Dransfeld C, Tsakoniatis I, Benedictus R. Co-cure joining of epoxy composites with rapidly UV-irradiated PEEK and PPS composites to achieve high structural integrity. *Compos. Struct.* 2020; 251:Article 112595.
2. Xiong X, Wang D, Wei J, Zhao P, Ren R, Dong J, Cui X. Resistance welding technology of fiber reinforced polymer composites: a review. *J. Adhes. Sci. Technol.* 2021; 35(15):1593-1619.
3. Ageorges C, Ye L, Hou M. Experimental investigation of the resistance welding for thermoplastic-matrix composites. Part I: Heating element and heat transfer. *Compos. Sci. Technol.* 2000; 60(7):1027-1039.
4. Deng S, Djukic L, Paton R, Ye L. Thermoplastic-epoxy interactions and their potential applications in joining composite structures - A review. *Composites Part A.* 2015; 68:121-132.
5. Campbell FC. *Manufacturing Processes for Advanced Composites*. Oxford: Elsevier Advanced Technology; 2003.
6. Tsiangou E, Teixeira de Freitas S, Fernandez Villegas I, Benedictus R. Ultrasonic welding of epoxy- to polyetheretherketone- based composites: Investigation on the material of the energy director and the thickness of the coupling layer. *J. Compos. Mater.* 2020; 54(22):3081-3098.
7. Fernandez Villegas I, van Moorleghem R. Ultrasonic welding of carbon/epoxy and carbon/PEEK composites through a PEI thermoplastic coupling layer. *Composites Part A.* 2018; 109:75-83.
8. Ageorges C, Ye L. Resistance welding of thermosetting composite/thermoplastic composite joints. *Composites Part A.* 2001; 32:1603-1612.
9. Zweifel L, Brauner C. Investigation of the interphase mechanisms and welding behaviour of fast-curing epoxy based composites with co-cured thermoplastic boundary layers. *Composites Part A.* 2020; 139:Article 106120.
10. ASTM. ASTM D5528-13(2021). Standard Test Method for Mode I Interlaminar Fracture Toughness of Unidirectional Fiber-Reinforced Polymer Matrix Composites. West Conshohocken (PA): ASTM International; 2021.

  doi:10.5075/epfl-298799_978-2-9701614-0-0